ISBN: 978-3-95450-227-1 ISSN: 2673-5490 doi:10.18429/JACoW-IPAC2022-MOPOPT032

IMPROVEMENT OF MATCHING CIRCUIT FOR J-PARC MAIN RING INJECTION KICKER MAGNET

T. Sugimoto*, K. Ishii, T. Shibata, S. Iwata, H. Matsumoto, KEK, Tsukuba, Japan

Abstract

This paper describes the improvements achieved in the impedance matching circuit for the 1.3 MW beam operation of the Japan Proton Accelerator Complex main ring injection kicker magnet. In this regard, the number of paralleled resistors was doubled, and the volume of each resistor was enlarged 2.6 times to lower the temperature of the resistors under the higher repetition rate pulse excitation. In addition, the resistor cylinders were filled with ceramic-based beads of 3 mm diameter to increase the heat conductivity. Moreover, an aluminum-made water-cooled heat sink was attached to the resistors directly, and an air-cooling fan was mounted on the side of the box containing the resistors. All resistors and their support structure in the matching circuit were replaced in May 2022. The temperature increment of resistors during continuous pulse excitation was measured using a thermography camera, and the measured value was compared with numerical calculations. Finally, the prediction results related to the beam image current obtained with the simulation model were discussed.

INTRODUCTION

J-PARC (Japan Proton Accelerator Complex) consists of three accelerators, a 400-MeV Linac, a 3-GeV Rapid Cycle Synchrotron (RCS), and a 30-GeV Main Ring (MR). The MR provides a high-intensity proton beam to the long baseline neutrino experiment (T2K) and the hadron experiments. In 2019, the beam intensity provided to the neutrino experiment was 495 kW corresponding to 2.56 $\times 10^{14}$ proton per pulse (ppp) for a repetition rate of 2.48 s [1]. However, a stable operation for high-intensity beams is required to achieve an accurate measurement of the neutrino oscillation and observe the neutrino CP violation. In particular, in the late 2020s, high intensity operation of 1.3 MW beam power will be achieved by shortening the repetition period from 2.48 sec to 1.16 sec and increasing the number of protons from 2.4 $\times 10^{14}$ to 3.34 $\times 10^{14}$ ppp [2, 3]. Including the margin, the hardware is developed to operate within a repetition period of 1 s. Proton beams extracted from the RCS were injected into the MR by four kicker magnets [4–6]. The harmonic number of the MR is nine. One RF bucket was left empty for the extraction kickers to ease the requirement of the field rise time. Four successive batches from the RCS were injected into the MR to fill 8 RF buckets spaced at 300 ns interval. Circulating bunches were deflected additionally by the residual field of the reflection pulses. It caused the coherent oscillation which induced the beam loss during the injection period. Thus, an impedance matching circuit should be implemented in the injection kicker magnet to reduce the reflection pulses. The circuit consists of a non-inductive ceramic resistor [7] and a high voltage ceramic capacitor. These elements are contained in the dedicated steel-made boxes. A maximum temperature of the resistor is recommended to operate within 150 °C to prevent degrading of the resistance. However, previous studies have suggested that the temperature of the resistor exceeded 350 °C during the continuous 1.3 MW operation [8, 9]. Therefore, a large diameter ceramic resistor should be developed to lower the temperature, and these larger ceramic resistors were installed into new boxes in May 2022. In this report, the new resistor and the matching circuit are detailed, and the temperature measurements are reported.

MATCHING CIRCUIT REPLACEMENT

Resistors

Figure 1 shows the equivalent circuit of the injection kicker magnet. The impedance matching resistor R_1 is connected to the kicker coil L_1 to reduce the reflection pulse. The resistance is 9.3 Ω, optimized by measuring the pulse shape [6]. Fifteen non-inductive ceramic resistors are connected in parallel (called "resistor-unit"). The resistors unit is contained in an individual box settled on the vacuum chamber (named the "matching box"). Resistors (R_2) and capacitors (C_2) are connected to the coil in parallel both to reduce the beam coupling impedance [4, 5] and to match the impedance for the high frequency region. The resistor electrodes were brazed at both ends of the conductive ceramics to avoid discharge [7]. The typical excitation current of the pulse is 2640 A, and the pulse width is 1.5 μsec. The pulse energy is approximately 100 J. A pulse was fed into the coil to deflect the orbit of 2 bunches to the circular orbit. The kicker magnet was excited in four times during the injection period to inject in total 8 bunches in the MR. When the circulating beam passes through the kicker aperture, an image current flows through the coil. Subsequently, the current flows in the matching circuit connected to the coil (i.e., R_1, R_2 and C_1). Therefore, the resistor R_1 is heated by both the excitation pulse current and the beam image current, while the resistor R_2 is heated only by the beam image current. The temperature rise of the resistor ΔT can be estimated as follows:

$$\Delta T = \frac{1}{N}\frac{Q_{pulse} + Q_{beam}}{hA} \quad (1)$$

$$= \frac{1}{NhA}\left(\int I^2(t)dt\frac{R}{T_{rep}} + \int E_b(t)dt\right) \quad (2)$$

where N is the number of resistors connected in parallel, Q_{pulse} is the power of the excitation pulse of the kicker magnet, Q_{beam} is the power of the beam image current, h is the

* takuya.sugimoto@j-parc.jp

ISBN: 978-3-95450-227-1 ISSN: 2673-5490 doi:10.18429/JACoW-IPAC2022-MOPOPT032

convective heat transfer coefficient, A is the surface area of the resistor, I(t) is the excitation current of the magnet, R is the total resistance of the resistors, T_{rep} is the repetition period, $E_b(t)$ is the pulse energy of the beam induced current. Note that the denominator NhA in Eq.(2) should be low to reduce ΔT.

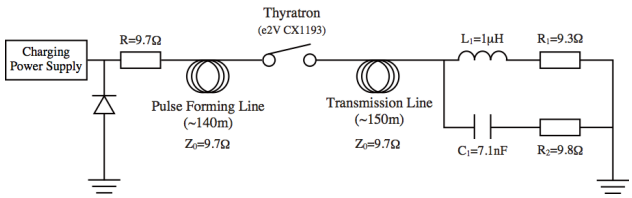

Figure 1: Equivalent circuit of the injection kicker system.

Several types of resistors were tested to select the size of the new resistor. The electrodes could not be brazed to the ceramic when the outer diameter was above 40mm. The reason was the heavy outgassing from the ceramic and the large porosity of the ceramic In contrast, outgassing from the ceramic with a diameter of 30 mm was acceptable for mass production. Moreover, two different length of the ceramic (170 mm and 200 mm) were fabricated and tested at a test stand in KEK. No discharge was observed for 170 mm after 1000 hours of operation, while arc discharge was observed for 200 mm. Therefore, the dimensions of the new resistor were an outer diameter of 30 mm and a length of 170 mm. The left side of Fig. 2 shows the ceramic resistors manufactured by a Japanese company [10]. The upper resistor is the original resistor, with an outer diameter of 20 mm and a length of 170 mm. The lower image represents the new resistor, with an outer diameter of 30 mm and a length of 170 mm. The electrodes are brazed directly at the both ends of the ceramic resistor to prevent discharging between the ceramic and the electrode [7]. In contrast, the electrodes of the original resistor are attached by the tightening pressure. The epoxy-type painting (black) is adopted instead of the silicone-type painting (red) to reinforce the bond between the ceramic and the electrode. As a result, the outer diameter increment enlarged the surface area 1.5 times. Moreover, the number of paralleled resistors increased from 15 to 30, and the total volume of the resistor was enlarged 2.6 times.

Cooling System

An aluminum-made water-cooled heat sink (named "Liquid Cold Plates" manufactured by Kawaso Texcel Co., Ltd. [11]) was attached to the resistor. In addition, ceramic-based beads with a diameter of 3 mm were placed in the resistor cylinder to improve the thermal conduction, as shown on the right side of Fig. 2. Three types of the diameter of the beads diameter (1 mm, 3 mm and 5 mm) and three types of different material (99.5% Al_2O_3, 95% Al_2O_3, and SiC) were tested. The results were compared with those from a ceramic rod reported in the previous studies [8, 9]. No clear differences were observed, however, the ceramic beads (ϕ3mm, 95% purity) presented the lowest cost.

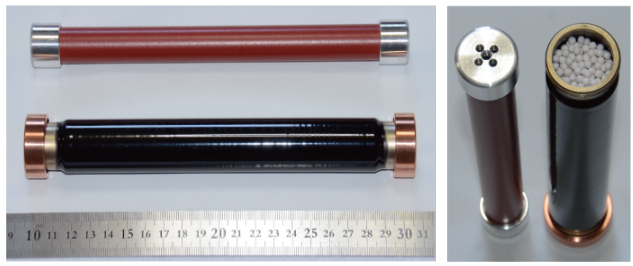

Figure 2: Ceramic resistors. Upper left: original resistor (ϕ20×L170mm); lower left: new resistor (ϕ30×L170mm), the electrodes were brazed directly onto the ceramic. Right: ceramic beads placed in the resistor.

Resistor Unit

Figure 3 shows the new resistor units. As shown in the figure, the resistor unit connected to the coil (called "coil side") consists of 30 resistors, and that connected to the capacitor (called "capacitor side") consists of 15 resistors. In a previous study, the maximum temperature of cylindrical placement was considered [8]. Moreover, grid placement was taken into account after the study. In particular, the comparison regarding the simulated maximum temperature showed no substantial differences. Therefore, grid placement was adopted to obtain a smaller unit. A current transformer (Pearson Model4997) was assembled to the coil side unit to measure the excitation current waveform. Subsequently, each unit was connected to the kicker coil. A total 240 resistors for the coil side and 120 resistors for the capacitor side were fabricated to connect to the eight kicker coils. Finally, customized heat sink was used to connect each resistor to remove the heat generated from the resistors.

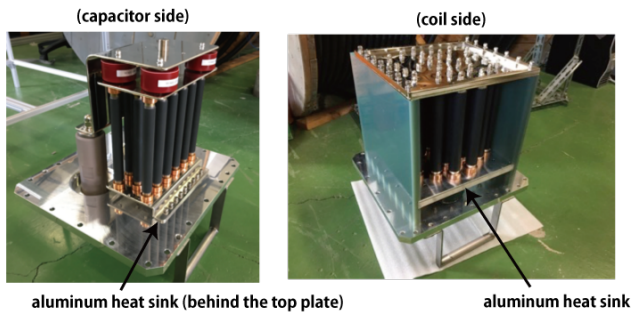

Figure 3: Resistor unit.

Assembly

Figure 4 shows the new matching circuit housing mounted on the vacuum chamber of the kicker magnet. All resistor units and their support structure were replaced in May 2022. Currently, no cooling fan was attached. No discharge was observed up to the charging voltage of 55 kV.

RESULTS

Figure 5 shows the surface temperature distribution of the new resistor unit of the coil side measured by a thermogra-

ISBN: 978-3-95450-227-1 ISSN: 2673-5490 doi:10.18429/JACoW-IPAC2022-MOPOPT032

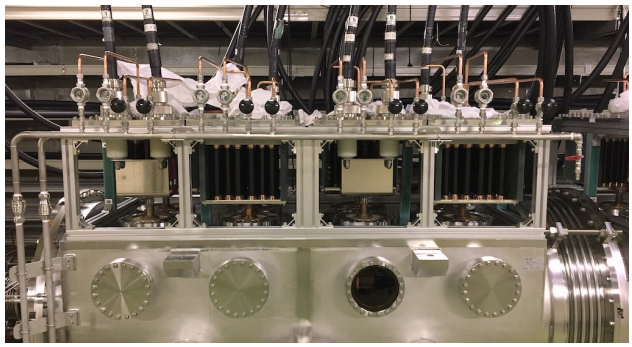

Figure 4: New matching circuit housing mounted on the vacuum chamber of the injection kicker magnet.

phy (FLIR E8) and a thermal label. In the measurement, the cooling fan was turned off to estimate the performance of the water-cooled heat sink. After 24 hours of continuous operation with an average power of 316 W (peak current: 2700 A, repetition cycle: 1.36 sec), a maximum temperature (T_{max}) of 100 °C was observed around the center of the resistor unit. The amount of heat removed by water was estimated as 145 W because the temperature difference between the cooling water inlet and outlet was 1.2 °C for a water flow rate of 7 L/min. A numerical simulation was performed to evaluate the temperature distribution and the maximum temperature T_{max} of the resistor. The water temperature in the heat sink was fixed to 30 °C. Moreover, the ceramic beads were modeled as a ceramic rod. The packing factor of the ceramic beads was assumed as 0.7 (i.e. closest packing). The thermal conductivity of the ceramic beads was assumed as 5 W/K/m. As the result of the simulation, a T_{max} = 90 °C was obtained through simulations. The temperature of the area where the thermal label was attached was 84 °C. Finally, the remaining discrepancies might be related to the material modeling of ceramic beads and the contact thermal resistance between beads.

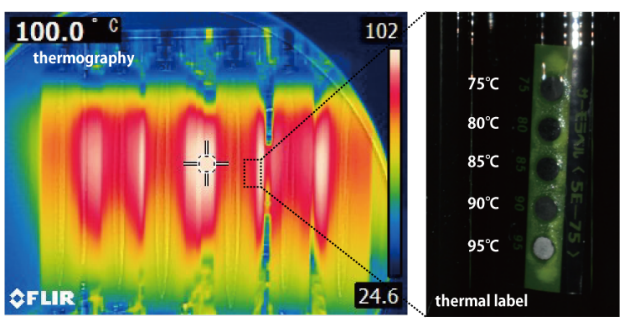

Figure 5: Resistor temperature measured by a thermography (left) and a thermal label attached on a resistor (right).

DISCUSSION

Resistor temperature for 1.3 MW continuous operation was estimated using the simulation model. Possible power dissipation on the resistor for the estimation was assumed as 1 kW (pulse operation: 400 W, and beam image current: 600 W). In a previous study, the amount of the heat dissipated from beam image current was estimated as 184 W. Moreover, we considered a safety factor of 3 to estimate the effect of the beam image current because the current waveform depended on the beam trajectory and the charge distribution of the beam bunch passing through the kicker magnet aperture. A 3D numerical model was created using the CST Studio Suite [12] to estimate the temperature increment for 1 kW power dissipation. A thermal fluid simulation relying on the CST Conjugate Heat Transfer (CHT) solver was performed to estimate T_{max}. The results shows that T_{max} = 180 °C (coil side, w/o cooling fan), T_{max} = 125 °C (coil side, wind speed v = 2 m/s), and T_{max} = 137 °C (capacitor side, w/o cooling fan). Thus, the operation might be continued until a weekly maintenance day, even if the cooling fan fails during operation.

CONCLUSION

In this study, an impedance matching circuit was developed to lower the surface temperature of the resistors during 1.3 MW operation of the J-PARC Main Ring Injection Kicker Magnet. In this regard, the number of resistors connected in parallel and their diameter was increased to increase the heat capacity and the surface area. Moreover, the cooling system was upgraded. For instance, an aluminum-made water-cooled heat sink was attached to the resistor. These resistors were filled with ϕ 3 mm alumina-made beads to improve the heat conduction, and the resistor temperature was measured during 24 hours of continuous pulse excitation. A T_{max} = 100 °C was observed for the average power of 316 W. A good agreement between the measurement and the numerical simulation was obtained. In addition, a simulation model was used to predict the resistor temperature during 1.3MW continuous operation. In particular, a temperature of less than 180 °C is expected for the coil side during the operation, even if the cooling fan fails. The resistor temperature for the capacitor side will be measured during the continuous high power operation scheduled in late 2022.

REFERENCES

[1] Y. Sato, "High Power Beam Operation of the J-PARC RCS and MR", in *Proc. IPAC'18*, Vancouver, Canada, Apr.-May 2018, pp. 2938–2942. doi:10.18429/JACoW-IPAC2018-THYGBF1

[2] T. Koseki, "Upgrade Plan of J-PARC MR - Toward 1.3 MW Beam Power", in *Proc. IPAC'18*, Vancouver, Canada, Apr.-May 2018, pp. 966–969. doi:10.18429/JACoW-IPAC2018-TUPAK005

[3] M. Yoshii *et al.*, "Present Status and Future Upgrades of the J-PARC Ring RF Systems", in *Proc. IPAC'18*, Vancouver, Canada, Apr.-May 2018, pp. 984–986. doi:10.18429/JACoW-IPAC2018-TUPAK011

[4] K. Fan, S. Fukuoka, H. Matsumoto, T. Sugimoto, and T. Toyama, "Coupling Impedance Study of the New Injection Kicker Magnets of the JPARC Main Ring", in *Proc. IPAC'12*,

ISBN: 978-3-95450-227-1 ISSN: 2673-5490 doi:10.18429/JACoW-IPAC2022-MOPOPT032

New Orleans, LA, USA, May 2012, paper THPPP003, pp. 3725–3727.

[5] K. Fan *et al.*, "Design and Test of Injection Kicker Magnets for the JPARC Main Ring", in *Proc. IPAC'12*, New Orleans, LA, USA, May 2012, paper THPPP004, pp. 3728–3730.

[6] T. Sugimoto, K. Fan, K. Ishii, and H. Matsumoto, "Upgrade of the Injection Kicker System for J-PARC Main Ring", in *Proc. IPAC'14*, Dresden, Germany, Jun. 2014, pp. 526–528. doi:10.18429/JACoW-IPAC2014-MOPME069

[7] T. Sugimoto, K. Fan, K. Ishii, H. Matsumoto, K. Abe, and S. Fukuoka, "Development of a Non-inductive Ceramic Resistor", in *Proc. IPAC'13*, Shanghai, China, May 2013, paper MOPWA004, pp. 669–671.

[8] T. Sugimoto, K. Ishii, H. Matsumoto, and T. Shibata, "Recent Improvements and Future Upgrades of the J-PARC Main Ring Kicker Systems", in *Proc. IPAC'19*, Melbourne, Australia, May 2019, pp. 4167–4170. doi:10.18429/JACoW-IPAC2019-THPTS028

[9] T. Sugimoto et al., "Performance of new termination resistors of J-PARC Main Ring injection kicker magnet", in Proc. PASJ'20, Japan, FRPP44 (in Japanese).

[10] Tokai Konetsu Kogyo Co., Ltd., https://www.tokaikonetsu.co.jp/english/index_en.html

[11] Kawaso Texcel Co., Ltd., https://www.kawaso-texcel.com/en/product/liquidcoldplate/index.html

[12] Computer Simulation Technology, https://www.cst.com/